Energy Landscapes of Nucleophilic Substitution Reactions: A Comparison of Density Functional Theory and Coupled Cluster Methods

MARCEL SWART,[1] MIQUEL SOLÀ,[2] F. MATTHIAS BICKELHAUPT[1]
[1]*Theoretische Chemie, Scheikundig Laboratorium der Vrije Universiteit, De Boelelaan 1083, NL-1081 HV Amsterdam, The Netherlands*
[2]*Institut de Química Computacional, Universitat de Girona, Campus Montilivi, E-17071 Girona, Catalunya, Spain*

Received 13 April 2006; Revised 24 May 2006; Accepted 26 June 2006
DOI 10.1002/jcc.20653
Published online 6 March 2007 in Wiley InterScience (www.interscience.wiley.com).

Abstract: We have carried out a detailed evaluation of the performance of all classes of density functional theory (DFT) for describing the potential energy surface (PES) of a wide range of nucleophilic substitution (S_N2) reactions involving, amongst others, nucleophilic attack at carbon, nitrogen, silicon, and sulfur. In particular, we investigate the ability of the local density approximation (LDA), generalized gradient approximation (GGA), meta-GGA as well as hybrid DFT to reproduce high-level coupled cluster (CCSD(T)) benchmarks that are close to the basis set limit. The most accurate GGA, meta-GGA, and hybrid functionals yield mean absolute deviations of about 2 kcal/mol relative to the coupled cluster data, for reactant complexation, central barriers, overall barriers as well as reaction energies. For the three nonlocal DFT classes, the best functionals are found to be OPBE (GGA), OLAP3 (meta-GGA), and mPBE0KCIS (hybrid DFT). The popular B3LYP functional is not bad but performs significantly worse than the best GGA functionals. Furthermore, we have compared the geometries from several density functionals with the reference CCSD(T) data. The same GGA functionals that perform best for the energies (OPBE, OLYP), also perform best for the geometries with average absolute deviations in bond lengths of 0.06 Å and 0.6°, even better than the best meta-GGA and hybrid functionals. In view of the reduced computational effort of GGAs with respect to meta-GGAs and hybrid functionals, let alone coupled cluster, we recommend the use of accurate GGAs such as OPBE or OLYP for the study of S_N2 reactions.

 J Comput Chem 28: 1551–1560, 2007

Key words: density functional theory; coupled cluster; nucleophilic substitution reaction

Introduction

The discovery in 1953 of the double stranded helical structure of DNA has led to several new insights on the origin and continuation of life.[1] One of the key features of the DNA structure comprises the hydrogen bonds between the different DNA base pairs, that are strong and specific and well understood by high-level theoretical analyses.[2–4] The process of DNA replication, i.e., the creation of an exact copy of one of the strands by fusing together DNA nucleotides, occurs with high fidelity, the origin of which is still under debate.[5,6] The basic reaction taking place in the DNA replication process is a nucleophilic substitution (S_N2) of the sugar moiety of the partly made strand (primer) on the phosphate group of the to-be-added nucleotide (see Scheme 1). The analysis of this S_N2 reaction is important not only for its own sake, but also as a starting point for achieving a complete understanding of the whole replication process in DNA.

Nucleophilic substitution reactions are usually associated with organic compounds, in many cases with halide anions as leaving group or nucleophile. Because of its importance for organic chemistry synthesis and the relative simplicity of intermediates, often involving highly symmetric structures, the S_N2 reaction has been the subject of a large number of theoretical investigations,[7] ranging from low-level semi-empirical to high-

This article contains supplementary material available via the Internet at http://www.interscience.wiley.com/jpages/0192-8651/suppmat

Correspondence to: F. M. Bickelhaupt; e-mail: fm.bickelhaupt@few.vu.nl

Contract/grant sponsors: HPC-Europa program of the European Union, The Netherlands Organization for Scientific Research (NWO)

Contract/grant sponsor: Spanish MEC; contract/grant number: CTQ2005-08797-C02-01/BQU

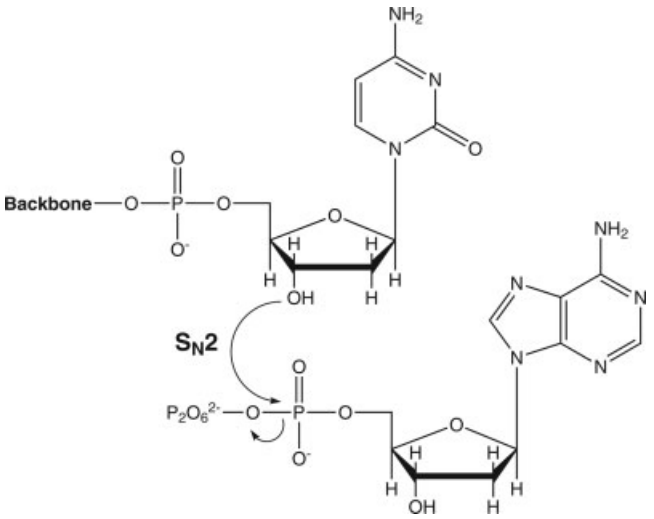

Scheme 1. S_N2 reaction taking place in the DNA replication process.

level coupled cluster studies with basis sets close to the basis set limit. The latter and also the related QCISD method have occasionally been used as benchmark for the assessment of the energy functionals used in density functional theory (DFT),[8–10] but usually only a limited number of DFT functionals has been tested.[11–18] The latter studies indicate a clear underestimation of the central barrier (if present) by standard pure DFT functionals (such as BP86[13,19,20]), which is usually improved upon by mixing in part of Hartree-Fock exchange in the hybrid functionals (e.g. B3LYP[21]). Interestingly, recent preliminary studies[11,13,14] indicated a considerable improvement of the reaction barriers, if more recent pure DFT functionals were used. Note also the good performance of the very recent M05 and M05-2X functionals for reaction barriers of hydrogen-transfer reactions.[22] Although the latter paper investigates the functionals for their general performance, in contrast to the current contribution that focuses and elaborates in more detail on the performance for S_N2 reactions, their conclusions support our more general conclusion (*vide infra*) that barriers/reaction energies are well described with modern DFT approaches, such as M05-2X, OPBE, and OLYP.

In this contribution, we report a systematic investigation of the performance of DFT functionals for describing the complete energy profile of S_N2 reactions, where the reference data have been taken from high-level theoretical investigations, in particular coupled cluster methods with (preferably) large basis sets that were taken from the literature. The comparison will provide valuable information regarding the question which DFT method should be used in studies on larger systems, such as present in the replication process of DNA. We divide the reference data into three sets (see Table 1): one in which coupled cluster (CCSD(T)) methods have been used both for computing the geometries of the stationary points and the energy (CC//CC, set A); one in which coupled cluster methods have been used in a single-point fashion to compute the energy based on structures that were obtained at a lower level of theory (CC//nonCC, set B); and one in which coupled cluster methods were used neither for computing geometries nor energies which instead were obtained at a lower level of ab initio theory (nonCC//nonCC, set C). In all cases, we use the nonextrapolated data, as far as they are available from the original data.

The study consists of two parts: in the first part, we look at the energetics and use strictly the geometry from the original papers. In the second part, we optimize the geometries with several density functionals and compare them with the best available CCSD(T) geometries.

Methods

All calculations were performed with the Amsterdam Density Functional (ADF)[23,24] program developed by Baerends and coworkers. The MOs were expanded in uncontracted sets of Slater-type orbitals,[25] which are of double-ζ quality (DZ), double-ζ quality augmented by one set of polarization functions (DZP), triple-ζ quality augmented by one set of polarization functions (TZP), triple-ζ quality augmented by two sets of polarization functions (TZ2P), and of quadruple-ζ quality augmented by four sets of polarization functions (QZ4P). In the energy calculations of the first part, all electrons were treated variationally. In the geometry optimizations of the second part, the core electrons were treated with the frozen core approximation[24] if possible, which was shown to have a negligible effect on the accuracy of the geometries[26] and relative energies.[27–31] An auxiliary set of s, p, d, f, and g STOs was used to fit the molecular density and to represent the Coulomb and exchange potentials accurately in each SCF cycle. In the first part, the energies for the different xc-functionals were calculated in a post-SCF fashion on orbitals and densities resulting from the local density approximation (LDA; Slater exchange and VWN[32] correlation); the influence of self-consistency on energy differences was previously shown to be small ($\sim$0.2 kcal/mol).[27–31]

The geometry optimizations were primarily performed with the ADF program, but for some problematic systems and/or the geometry optimizations with meta-GGA and hybrid functionals (*vide infra*) the QUILD program[33,34] was used; for the latter functionals (for which the analytical gradient is not available in ADF) the gradients were evaluated through numerical differentiation of the energy. The QUILD program[33,34] serves as a wrapper around the ADF program, in which the geometry optimization is being handled by QUILD and ADF serves only to deliver the DFT energy and gradient; the use of modified delocalized coordinates[34] within QUILD enhances the convergence of the geometry optimizations. The convergence criterium for the gradient was in all cases set to $1.0 \cdot 10^{-5}$ au.

Table 1. Methods Used in the Three Data Sets (A, B, C) for Obtaining Energy and Geometry.

Set	Method	Energy	Geometry
A	CC//CC	CCSD(T)	CCSD(T)
B	CC//nonCC	CCSD(T)	Other ab initio
C	nonCC//nonCC	Other ab initio	Other ab initio

DFT Functionals

The many DFT functionals that have been constructed over the past twenty years can be grouped into the following four classes.[35] (1) For the simplest functionals the energy depends only on the charge density ρ. This is termed the LDA. (2) An improvement results when the energy depends also on the density gradient $\bigtriangledown\rho$, i.e., the generalized gradient approximation (GGA). (3) For the meta-GGA functionals the energies depend also on the Laplacian of the density $\bigtriangledown^2\rho$ and/or the orbital kinetic energy. (4) Lastly, there are the so-called hybrid functionals that include a portion of exact (Hartree-Fock) exchange.

DFT functionals typically have exchange and correlation parts that are constructed independently. The most popular pure GGA exchange functional is Becke88,[19] while frequently used GGA correlation functionals are those from Perdew[20] or from Lee, Yang, and Parr (LYP)[36]. Their combination for exchange and correlation gives the Becke-Perdew (BP86) or BLYP functionals.

DFT functionals can also be divided into empirical and nonempirical ones. Nonempirical functionals like PBE[37] are derived by theoretical considerations and contain physical constants as parameters. Empirical functionals have been optimized for sets of molecules mimicking the G2-set like HCTH,[38–40] which contains a set of 15 fitting parameters, or B3LYP, containing 3 fitting parameters. These empirical functionals may function well for molecules within the set that they were fitted to, but may fail for others.[41]

The newly developed GGA exchange functional OPTX[42] gives an improvement over the widely used Becke88.[11,14] When combined with LYP it competes with the widely used B3LYP hybrid-GGA functional for the electronic description of organic molecules,[43,44] but its performance appeared less satisfactory for the spin states of transition metal complexes.[27] Promising results have been obtained by combining OPTX with PBE correlation (OPBE), which not only predicts correctly the spin ground states of iron complexes,[27] but also performs well for other systems and properties.[14] The OPTX functional may also be combined with the new meta-GGA correlation functional LAP3[45] (to give OLAP3); although the LAP3 parameters were obtained in combination with Becke88 exchange, the same parameters are used for OLAP3.[11]

Other new meta-GGAs are those developed by Filatov-Thiel (FT97),[46] van Voorhis-Scuseria (VS98),[47], Krieger-Chen-Iafrate-Savin (KCIS),[48] Becke (Becke00),[49] and Perdew's latest (and most accurate) TPSS;[41,50] the TPSSh functional includes 10% exact exchange. The new M05 and M05-2X functionals, which were recently[22] shown to perform well for barriers of hydrogen-abstraction reactions, are not yet available in the ADF program, and could therefore not be considered in this study.

Results

The typical energy profile for an S_N2 reaction is shown in Figure 1. After initial formation of a reactant complex (RC), the reaction proceeds via a transition state (TS) to a product complex (PC), and finally, the products (P). In many (if not most) cases, the nucleophile and leaving group are anionic species, which leads to relatively stable reactant and PCs because of substantial donor–acceptor orbital interactions as well as electrostatic ion-dipole interactions. This causes the occurrence of the well-known double-well potential energy surface (PES) along the reaction coordinate (Fig. 1). This PES is characterized by two pronounced minima, associated with RC and PC that are interconverted through the TS for S_N2.

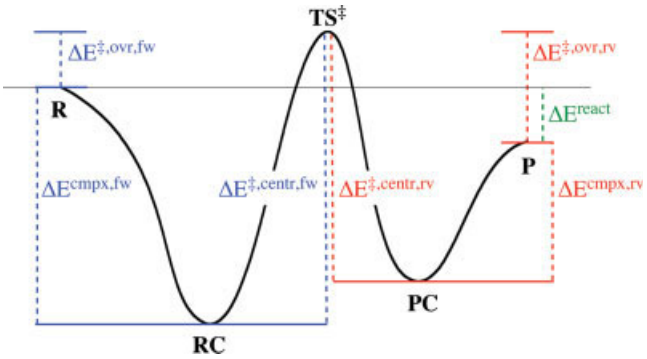

Figure 1. Energy profile for standard S_N2 reactions. [Color figure can be viewed in the online issue, which is available at www.interscience.wiley.com.]

As a consequence, the energy profile involves two important energy quantities regarding the barrier: (i) the central barrier, which is the difference in energy between TS and RC and (ii) the overall barrier, which is the difference between TS and separate reactants. Note that the latter may in principle (and does so in many cases) adopt negative values.

The overall barrier is decisive for the rate of chemical reactions in the gas phase, in particular, if they occur under low-pressure conditions in which the reaction system is (in good approximation) thermally isolated (see Refs. 51, 52). The central barrier becomes decisive in the high-pressure regime, when termolecular collisions are sufficiently efficient to cool the otherwise rovibrationally hot RC, causing it to be in thermal equilibrium with the environment. It may be tempting to conceive the central barrier of the gas-phase reaction as the barrier of the same process in solution. We stress, however, that this is not in general the case, because differential solvation of RC and TS can affect the barrier height substantially, even to the extent that relative heights of barriers for competing processes can be inverted (see, for example, Refs. 53, 54 and references cited therein).

In the case of a nonidentity reaction, in which the nucleophile and leaving group differ, the energy profile of the forward reaction differs, in general, from that of the reverse reaction. Thus, the complexation energy of the RC ($\Delta E^{\mathrm{cmpx,fw}}$ *vs.* $\Delta E^{\mathrm{cmpx,rv}}$; see Fig. 1) or central barrier ($\Delta E^{\ddagger,\mathrm{centr,fw}}$ *vs.* $\Delta E^{\ddagger,\mathrm{centr,rv}}$) are not the same for the forward and reverse reactions. In all cases, we examine both the forward and the reverse reaction.

We have measured the performance of the different DFT functionals by looking at the absolute values of the deviations of computed DFT energies from the CCSD(T) reference energies. The DFT energies were obtained using the same geometry as reported in the original studies. We examine the mean absolute deviations (MAD) in the following energy terms which together determine the energy profile of the S_N2 reaction (see Fig. 1 for their definition): (i) the complexation energy of the RCs ΔE^{cmpx}; (ii) the central barrier $\Delta E^{\ddagger,\mathrm{centr}}$; (iii) the overall barrier $\Delta E^{\ddagger,\mathrm{ovr}}$;

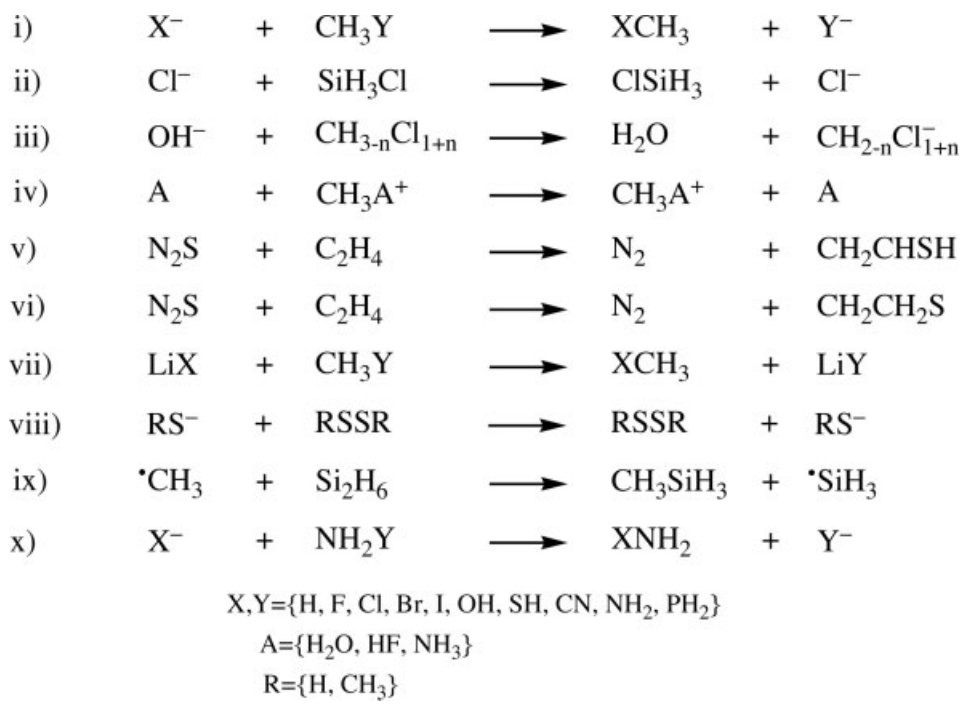

Scheme 2. S_N2 reactions considered in this study (see Tables S1–S3).

and (iv) the reaction energy ΔE^{react}. The overall performance P_E of a DFT functional is then obtained by taking the average of these four energy differences:

$$P_E = \left[\text{MAD}\left(\Delta E^{\text{react}}\right) + \text{MAD}\left(\Delta E^{\text{cmpx}}\right) + \text{MAD}\left(\Delta E^{\ddagger\text{centr}}\right) + \text{MAD}\left(\Delta E^{\ddagger\text{ovr}}\right)\right]/4 \quad (1)$$

Energetics of Benchmark Sets A, B, and C

Tables S1–S3 in the supporting information contain the CCSD(T) benchmark data for the energy profiles of the reactions in the three sets of reference data (A, B, and C, see Table 1) taken from the literature.[13,15,55–75] Each of the original articles are referred to by the letter of the reference set plus a number, e.g., A1 for Ref. 55 (see Table 1 and Tables S1–S3). If possible, the energies are used without zero-point vibrational energy (ZPE) correction, to enable a proper comparison with the DFT energies (which are also without ZPE correction). A schematic drawing of all reaction types considered is given in Scheme 2.

It is interesting to see the differences within the reference data from different studies on the same system, e.g., for the parent chloride + methylchloride reaction, a variation in the complexation energy of about 0.7 kcal/mol is observed along the studies **A3**,[68] **A6**,[67] **B1**,[13] **C1**,[65] and **C3**,[63] which probably results from differences in the methodology [CCSD(T) vs. QCISD(T) vs. G2(+)] as well as the extrapolation procedure used in the **A6**[67] paper. The differences for the fluoride + methylchloride system along papers **A1**,[55] **A5**,[62], and **A7**,[56,58] on the other hand, are more likely to result from differences in basis-set size. The most accurate results using a quadruple-ζ basis (**A5**)[62] show energies that are in between those from using a double-ζ (aug-ccpVDZ, **A7**)[56,58] and those from a triple-ζ basis (TZ2Pf+diff, **A1**).[55] QCISD(T) results[65] obtained with a large basis set resemble the double-ζ CCSD(T) values. As such, the most accurate data can be used to give an estimate for the accuracy of the lower-level basis set CCSD(T) data. Note that the quadruple-ζ energies are closer to the energies obtained with the double-ζ than to those obtained with the triple-ζ basis set. The mean absolute deviation relative to the quadruple-ζ energies is 2.2 kcal/mol for TZ2Pf+diff, but only 0.7 kcal/mol for the smaller aug-cc-pVDZ basis (see Table S1). However, with the double-ζ basis the geometries of the intermediates deviate more from the high-level quadruple-ζ results. In the RC, for example, the C—Cl and C—F distances in the TZ2Pf+diff basis have a mean absolute deviation of 0.6 pm from the quadruple-ζ data, while in the aug-cc-pVDZ basis it is 2.7 pm (data not shown in Tables). For the fluoride + methylfluoride system, similar differences of up to 1.1 kcal/mol occur along studies **A1**,[55] **A4**,[73] **A6**,[67] **B4**,[67] **C1**,[65] and **C3**[63] (see Tables S1–S3).

A summary of the accuracy of DFT functionals is reported in Table 2. The best functionals per class are LDA, OPBE (GGA), OLAP3 (meta-GGA), and mPBE0KCIS (hybrid), with overall performance P_E values [see eq. (1)] for set A of 7.2, 2.9, 2.3, and 2.2 kcal/mol respectively. In Table 2, for each reference paper the P_E value is given for the best functional within each of the four classes, LDA, GGA, meta-GGA, and hybrid DFT; also given is the average over all reactions within these papers, the complete data for all DFT functionals are provided in the supporting information. The most remarkable conclusion from this Table is the good performance of DFT with respect to the coupled-cluster benchmark data. The best functionals have an overall performance P_E of about 2 kcal/mol.

Table 2. Overall Performance P_E (in kcal/mol) for Best DFT Functionals and Other ab initio Methods.

Set	Ref.	Type[a]	nr.[b]	RHF	MP2	LDA	GGA[c]	Meta-GGA[d]	Hybrid DFT[e]
paper A1[f]	*55*	*i*	*7*	*7.0*[g]	*1.0*[h]	9.0	3.8 (g1)	2.5 (m1)	2.9 (h1, h2)
paper A2[i]	*69*	*i*	*1*	*3.4*[g]	*0.8*[h]	5.0	1.8 (g2)	2.2 (m1)	0.6 (h3)
paper A3[i]	*61,68*	*i*	*1*			4.8	1.0 (g2)	1.4 (m2)	0.6 (h4)
paper A4[i]	*72*	*i*	*1*	*4.5*	*0.6*	6.7	1.8 (g1,g3)	1.3 (m1)	0.8 (h3)
paper A5[i]	*62*	*i*	*1*			6.2	2.1 (g1)	2.2 (m1)	1.5 (h4)
paper A6[i]	*67*	*i*	*3*			5.5	1.8 (g2)	1.8 (m1)	0.6 (h3)
paper A7[j]	*56,58*	*i*	*1*			7.0	2.1 (g1)	2.0 (m1)	1.6 (h4)
paper A8[k]	*57*	*i*	*2*			6.9	1.0 (g2, g4)	0.8 (m3)	0.8 (h5, h6)
average set A			*17*			*7.2*	*2.9* (*g1*)	*2.3* (*m1*)	*2.2* (*h1, h4*)
paper B1[i]	*13*	*i,ii*	*2*	*3.5*	*0.6*	4.0	1.3 (g5)	1.6 (m4)	0.5 (h7)
paper B2[i]	*70*	*i*	*1*	–	*0.5*	6.0	1.6 (g1)	2.3 (m5)	0.5 (h4)
paper B3[i]	*60*	*iii*	*5*	*8.9*	*2.2*	7.1	1.5 (g2)	1.4 (m6)	1.8 (h8)
paper B4[i]	*67*	*i*	*6*	–	–	5.4	2.0 (g2, g5)	1.5 (m1)	1.1 (h4)
paper B5[i]	*71*	*iv*	*3*	–	*1.2*	2.7	1.4 (g2)	1.4 (m7)	0.9 (h7)
paper B6[l]	*75*	*v,vi*	*2*	–	*3.2*	11.3	4.9 (g1)	5.3 (m8)	2.6 (h7)
paper B7[i]	*74*	*vii*	*10*	–	–	5.9	3.4 (g5)	3.5 (m1)	1.9 (h7)
paper B8[l]	*59*	*viii*	*3*	–	*1.9*	5.9	1.4 (g2, g3)	1.1 (m1)	0.8 (h10, h11)
paper B9[j]	*66*	*ix*	*2*	–	–	11.2	1.0 (g6)	1.1 (m5)	0.6 (h1)
average set B			*34*	–	*2.7*[m]	*7.0*	*3.3* (*g1, g5*)	*3.4* (*m1*)	*2.4* (*h4, h12*)
paper C1[i]	*65*	*i*	*4*	–	–	5.9	2.1 (g2)	1.8 (m1)	0.6 (h3)
paper C2[i]	*72*	*i*	*1*	–	–	5.7	1.9 (g1)	2.2 (m6)	1.1 (h4)
paper C3[i]	*63*	*i*	*4*	–	–	5.6	1.7 (g1)	1.3 (m1)	0.8 (h3)
paper C4[i]	*64*	*x*	*4*	–	–	7.4	2.6 (g1)	1.4 (m1)	1.1 (h4)
average set C			*13*	–	–	*6.3*	*2.2* (*g1*)	*1.5 (m1)*	*1.1* (*h4*)

[a]Type of reactions in paper (see Scheme 2).
[b]Number of reactions in paper.
[c]In parentheses the best performing GGA functional, g1: OPBE, g2: HCTH/407, g3: HCTH/93, g4: HCTH/147, g5: OPerdew, g6: BOP.
[d]In parentheses the best performing Meta-GGA functional, m1: OLAP3, m2: FT97, m3: KCIS-modified, m4: mPBEKCIS, m5: Becke00, m6: BLAP3, m7: VS98, m8: PKZB.
[e]In parentheses the best performing Hybrid functional, h1: B1PW91, h2: O3LYP, h3: BHandH, h4: mPBE0KCIS, h5: B97-1, h6: mPBE1KCIS, h7: PBE0, h8: B3LYP, h9: B1LYP, h10: KMLYP, h11: mPW1K, h12: mPW1PW.
[f]DFT results using TZ2P basis.
[g]At the RHF optimized geometry.
[h]At the MP2 optimized geometry.
[i]DFT results using QZ4P basis.
[j]DFT results using TZP basis.
[k]DFT results using DZ basis.
[l]DFT results using DZP basis.
[m]Excluding papers B4, B7, and B9, for which there are no MP2 data available.

The most important set of reference data is the first one (set A, see Table 1), where coupled cluster methods have been used both for obtaining the geometry and the energy (CC//CC). For this set, the best functionals with an overall performance of 2.2–2.3 kcal/mol (see Tables 2 and S4) are OLAP3, mPBE0KCIS, and B1PW91. The best GGA functional (OPBE) is only 0.7 kcal/mol less accurate than these three with an overall performance P_E [see eq. (1)] of 2.9 kcal/mol. This is a very good performance, especially considering the reduced computational effort needed in comparison with the more elaborate meta-GGA and hybrid functionals, let alone the coupled cluster calculations.

The second set of reference data (set B, see Table 1) involves studies with coupled cluster energies on non-coupled cluster geometries (CC//nonCC). The results for the different functionals are similar to those found for the CC//CC set: the best one overall remains the mPBE0KCIS hybrid functional with an overall performance P_E [see eq. (1)] of 2.4 kcal/mol (see Table 2). The best performing GGA functionals (OPBE, OPerdew) follow closely with values of 3.3 kcal/mol (see Tables 2 and S5), and are now better than the best meta-GGA functional (OLAP3). Also for the third set (set C, nonCC//nonCC, see Table 1), which does not involve coupled cluster results, we find the same trend in (good) perform-

ance along the various density functionals for describing the energy profiles of the reference reactions (see Tables 2 and S6). The best GGA, meta-GGA, and hybrid functionals all agree excellently with the benchmark data, showing overall performance P_E [see eq. (1)] values between 1.1 and 2.2 kcal/mol (see Tables 2 and S6).

All of the above reported performances are likely to be influenced by the basis sets used. The performance of DFT functionals is much better (see Table 2) when a basis set close to the basis set limit has been used both in the reference study (**A2**–**A6**, see Table S1) and our DFT calculations, than when a smaller basis set was used in the literature CCSD(T) study (**A1**, **A7**–**A8**). When leaving out the benchmark studies employing smaller basis sets (i.e., taking into account only reactions **A2**–**A6**), the overall performance P_E of the DFT functionals improves; the best DFT functionals per class now have P_E values of 5.6 (LDA), 2.1 (OPBE), 1.8 (OLAP3), and 1.1 (mPBE0KCIS) kcal/mol.

Also given in Table 2 are the overall performance P_E [see eq. (1)] of RHF and MP2 for those reactions for which they were available. Although they seem to perform well for set A, the comparison with the DFT functionals is unfair: the RHF and MP2 energies have been obtained at their own optimized geometry, which may deviate largely from the reference CCSD(T) structure that has been used for the DFT functionals in the present study. For example, for the chloride + methylbromide reaction of paper **A2**,[69] the C—Br distance in the RHF or MP2 TS structure deviates by about 0.03 Å from the CCSD(T) structure, while the C—Cl distance even differs by 0.04 (MP2) and 0.12 Å (RHF). For normal bond distances, these differences are usually much smaller, i.e., less than 0.01 Å for MP2, and around 0.03 Å for RHF.[76] Therefore, as not only the method for obtaining the energy (RHF/MP2 *vs.* DFT) changes but also the geometries, it is impossible to directly compare the DFT performance with the performance for RHF or MP2, and, thus, no further comparison with RHF or MP2 will be made for the CC//CC set.

For the CC//nonCC set (set B, see Table 1), where the majority of the papers used MP2 for obtaining the geometry, we were able to compare our DFT data with MP2 (and sometimes the RHF) results (see Table 2). The accuracy of MP2 lies in these cases in between that of the best hybrid functional on one hand and those of the best GGA and meta-GGA functionals on the other hand (see Tables 2 and S5). This shows up also for its overall performance P_E (2.7 kcal/mol, see Table 2) that is slightly larger than that of PBE0/mPBE0KCIS (2.4 kcal/mol, see Table S5), and slightly lower than that of OPBE/OPerdew (3.3 kcal/mol) or OLAP3 (3.4 kcal/mol). The RHF results are comparable to those of LDA (see Tables 2 and S5).

Special Cases

The study by Uggerud (**B5**)[71] is special in that it is the only one that involves cationic species; apart from papers **B6**,[75] **B7**[74] and **B9**[66] that involve neutral species, all other papers deal with anionic species. The performance of DFT functionals to reproduce the energy profile of **B5** is good, with an overall performance P_E [see eq. (1)] of 2.7 kcal/mol (LDA) or less (data not shown in Table). For the neutral reactions of paper **B6**,[75] the pure DFT functionals perform less, which might be related to the difference in and quality of the (DZP) basis set used. For the CC//CC set A (see Table 1), a similar trend was observed (see Table 2). For the one paper (**B9**[66]) that deals with radical systems, all DFT methods (except LDA) perform well (data not shown in Table).

Table 3. Components of Overall Performance P_E for Set A (in kcal/mol) for Best Energy Functionals per DFT Class.

		Overall	ΔE^{cmpx}	$\Delta E^{\ddagger,centr}$	$\Delta E^{\ddagger,ovr}$	ΔE^{react}
LDA	*LDA*	7.23	6.77	6.49	13.01	2.66
OPBE	*GGA*	2.94	3.14	3.69	2.71	2.21
HCTH/93	*GGA*	3.13	2.41	4.14	3.38	2.60
OLAP3	*meta-GGA*	2.28	2.59	2.11	2.19	2.24
BLAP3	*meta-GGA*	3.57	1.63	4.92	5.47	2.28
mPBE0KCIS	*hybrid DFT*	2.22	2.06	1.85	2.67	2.31
BIPW91	*hybrid DFT*	2.23	1.99	2.23	2.19	2.51

MAD of Complexation Energy, Overall and Central Barrier, and Reaction Energy

In Table 3, we report, for the best functional of each DFT class, the MAD over all reactions studied, individually for each of the following energy terms: (i) the complexation energy ΔE^{cmpx}, (ii) the overall barrier $\Delta E^{\ddagger ovr}$, (iii) the central barrier $\Delta E^{\ddagger centr}$, and (iv) the reaction energy ΔE^{react}. For LDA, the overall performance P_E is dominated by the errors in the overall barrier (13.0 kcal/mol) and the reaction energy (2.7 kcal/mol), which are much higher cq. lower than the overall performance P_E of 7.2 kcal/mol (see Table 3). The spread is much smaller for the (best performing) GGA, meta-GGA, and hybrid functionals (see Table 3). For the GGA functionals, the error is largest for the central barrier (3.7 and 4.1 kcal/mol), and smallest for the reaction (OPBE, 2.2 kcal/mol), or complexation energy (HCTH/93, 2.4 kcal/mol).

The smallest error of the OLAP3 (meta-GGA) functional is for the central barrier (MAD value 2.1 kcal/mol, see Table 3) as reported earlier,[11,14] and the largest error is for the complexation energy (MAD value 2.6 kcal/mol). The second-best meta-GGA functional, BLAP3,[45] performs well for the complexation (MAD value 1.6 kcal/mol) and reaction energy (MAD value 2.3 kcal/mol), but shows larger errors for the barriers (MAD values of 4.9 and 5.5 kcal/mol, see Table 3). The overall performance P_E of the best-performing hybrid functionals benefits mainly from their performance for the complexation energy (MAD values about 2.0 kcal/mol, see Table 3) and the central barrier (MAD value 1.8–2.2 kcal/mol), and show some larger errors for the overall barrier (MAD value 2.2–2.7 kcal/mol, see Table 3) or the reaction energy (MAD value 2.3–2.5 kcal/mol, see Table 3).

In Table4, we report for each of the four DFT classes, the best performing functional for each separate component of the overall performance. Interestingly, the best performing GGA functional for the overall performance P_E (OPBE)[14] is also the best performing for three of the four components with MAD values of 2.2 (ΔE^{react}), 2.7 ($\Delta E^{\ddagger,ovr}$), and 3.7 ($\Delta E^{\ddagger,centr}$) kcal/mol (see Table 4); only for the complexation energy is OPBE not the best one (MAD value ΔE^{cmpx} OPBE 3.1 kcal/mol, see Table S4). However, in that case the difference with

Table 4. Best DFT Functional per Class for the Four Components of the Overall Performance P_E (in kcal/mol).

	ΔE^{cmpx}	$\Delta E^{\ddagger,centr}$	$\Delta E^{\ddagger,ovr}$	ΔE^{react}
LDA	6.77	6.49	13.01	2.66
GGA[a]	2.11 (g1)	3.69 (g2)	2.71 (g2)	2.21 (g2)
meta-GGA[b]	1.63 (m1, m2)	2.11 (m3)	2.19 (m3)	2.16 (m4)
hybrid DFT[c]	1.75 (h1)	1.85 (h2)	2.19 (h3)	2.21 (h4)

[a]In parentheses the best performing GGA functional, g1: BOP, g2: OPBE.
[b]In parentheses the best performing Meta-GGA functional, m1: BmTau1, m2: BLAP3, m3: OLAP3, m4: mPBEKCIS.
[c]In parentheses the best performing Hybrid functional, h1: KMLYP, h2: mPBE0KCIS, h3: B1PW91, h4: mPBE1KCIS.

the best GGA functional (BOP) is still only 1.0 kcal/mol (MAD value ΔE^{cmpx} BOP 2.1 kcal/mol, see Tables 4 and S4). The OLYP functional is another GGA functional that performs reasonably well for all four components of the overall performance. For the hybrid functionals, there is no one that is equally well on (almost) all fronts (see Tables 4 and S4): for each of the four components there is a different functional that performs best.

Contributions of Exchange and Correlation to the Energy Profile

The results for the fluoride + methylfluoride reaction of paper **A4**[73] have been used as reference data in a study by Gritsenko et al.,[12] in which they used multi-reference configuration interaction (MRCI) to provide the charge density that was subsequently used to obtain the true Kohn-Sham exchange (E_x) and correlation (E_c) energies for the intermediates. From the difference between the RC and TS energies, they obtained the contributions of exchange and correlation to the central barrier of 25.7 kcal/mol, which were found to be 28.9 (E_x) and −3.2 (E_c) kcal/mol. In their study, these values were compared with the ones obtained from three popular pure DFT functionals (BP86, BLYP, and PW91), which all showed a severe underestimation of the exchange part.

We repeated the calculations to include more DFT functionals in the comparison. In Table5, we report the results from our calculations with the TZ2P basis, of similar size as the triple-ζ basis that was used in the MRCI calculation. For the three popular functionals, i.e., BP86, BLYP, and PW91, the energies from LDA densities are reasonably similar to those from the MRCI density, e.g. with severe underestimation of the exchange part. This is improved upon by functionals that include OPTX exchange, which raises the exchange contribution by about 4 kcal/mol. Including a portion of exact exchange further increases this contribution; the larger the portion of exact exchange, the larger the contribution of the exchange. Therefore, it is no surprise that KMLYP, which has one of the largest contributions of exact exchange, shows the largest contribution of exchange energy to the central barrier. However, there is a trade-off: KMLYP is neither the best hybrid functional for the overall performance P_E, nor even for the central barriers in the CC//CC set (see Tables 4 and S4).

Table 5. Contributions (in kcal/mol) of Kohn–Sham DFT Exchange and Correlation Functionals to the Central Barrier of $F^- + CH_3F$.

		$E[\rho_{MRCI}]$[a]			$E[\rho_{LDA}]$[b]			$E[\rho_{OPBE}]$[c]		
		E_x	E_c	E_{xc}	E_x	E_c	E_{xc}	E_x	E_c	E_{xc}
KS		28.87	−3.19	25.68	–	–	–	–	–	–
LDA	*LDA*	–	–	–	13.26	0.19	13.45	15.25	0.29	15.54
OPBE	*GGA*	–	–	–	17.29	−0.28	17.00	19.89	−0.19	19.70
OLYP	*GGA*	–	–	–	17.29	−0.92	16.36	19.89	−0.95	18.94
PW91	*GGA*	12.96	0.38	13.34	14.03	−0.32	13.70	16.26	−0.24	16.02
BP86	*GGA*	13.58	−0.05	13.53	14.40	−0.77	13.64	16.67	−0.73	15.95
BLYP	*GGA*	13.58	−0.82	12.76	14.40	−0.92	13.48	16.67	−0.95	15.73
OLAP3	*meta-GGA*	–	–	–	17.29	2.05	19.34	19.89	2.20	22.09
TPSS	*meta-GGA*	–	–	–	13.13	−0.10	13.02	15.45	−0.02	15.43
FT97	*meta-GGA*	–	–	–	15.30	−2.57	12.73	17.73	−2.71	15.02
KMLYP	*hybrid DFT*	–	–	–	25.51	−0.31	25.20	27.85	−0.26	27.59
BHandH	*hybrid DFT*	–	–	–	24.26	−0.92	23.34	26.56	−0.95	25.61
mPW1K	*hybrid DFT*	–	–	–	23.21	−0.32	22.88	25.62	−0.24	25.38
mPBE0KCIS	*hybrid DFT*	–	–	–	19.60	0.11	19.71	21.96	0.20	22.16
B1PW91	*hybrid DFT*	–	–	–	19.62	−0.32	19.29	21.97	−0.24	21.74
B3LYP	*hybrid DFT*	–	–	–	17.38	−0.71	18.94	20.80	−0.71	20.09
O3LYP	*hybrid DFT*	–	–	–	19.65	−0.71	16.67	22.29	−0.71	21.58
TPSSh	*hybrid DFT*	–	–	–	15.34	−0.10	15.24	17.69	−0.02	17.67

[a]post-SCF from MRCI density, from ref. 12.
[b]post-SCF from LDA/TZ2P density.
[c]post-SCF from OPBE/TZ2P density.

Table 6. Mean Absolute Deviations in Geometries (Å, deg) for Various Density Functionals Compared to CCSD(T).

Functional	R_{all}	$R_{R,P}$	$R_{RC,PC}$	R_{TS}	θ_{all}	$\theta_{R,P}$	$\theta_{RC,PC}$	θ_{TS}	P_G
OLYP	0.058	0.006	0.089	0.036	0.567	0.156	0.439	1.636	0.033
OPBE	0.063	0.011	0.108	0.018	0.661	0.447	0.645	1.066	0.042
mPBE0KCIS	0.046	0.007	0.037	0.088	1.313	0.327	0.604	5.085	0.060
OLAP3	0.132	0.007	0.206	0.084	0.515	0.138	0.208	2.063	0.068
RevPBE	0.089[a]	0.010	0.135	0.051[a]	3.039[a]	0.146	4.668	2.941[a]	0.270
RPBE	0.092[a]	0.011	0.139	0.052[a]	3.001[a]	0.159	4.640	2.730[a]	0.276
BP86	0.096[a]	0.008	0.137	0.077[a]	3.497[a]	0.150	5.566	2.550[a]	0.336
LDA	0.098[a]	0.014	0.155	0.039[a]	3.450[a]	0.487	5.039	3.708[a]	0.338
PBE	0.120[b]	0.007	0.195	0.020[b]	5.104[b]	0.150	8.362	0.559[b]	0.612
mPBE	0.123[b]	0.008	0.198	0.024[b]	5.084[b]	0.142	8.339	0.503[b]	0.625
mPW	0.122[b]	0.008	0.197	0.024[b]	5.132[b]	0.152	8.389	0.716[b]	0.626
BLYP	0.134[a]	0.017	0.212	0.059[a]	5.376[a]	0.311	8.682	3.159[a]	0.720

See eq. 2 for P_G.
[a]Failed to optimize the TS for $F^- + CH_3Cl$ in TZP basis.
[b]Failed to optimize the TS for $F^- + CH_3Cl$ in TZP and QZ4P basis.

Table 5 also suggests a reason for the good performance of the OLAP3 and mPBE0KCIS functionals, i.e., the best performing meta-GGA and hybrid functionals. For both the correlation contribution is positive, while it should have been negative, that is, the correlation functionals behave effectively as quasi-exchange.

The best performing GGA functional for the contributions of exchange and correlation to the central barrier of $F^- + CH_3F$ is again OPBE (see Table 5). To investigate the influence of the use of LDA densities, we also performed the calculations on this system evaluated with a self-consistent OPBE density. The effect on the contribution of correlation is virtually negligible, with changes in the order of 0.15 kcal/mol or less (see Table 5). However, the contribution of exchange is more sensitive to the density used for evaluating the functional, showing changes of 2.0–3.5 kcal/mol for the different functionals.

Interestingly, the variations in overall performance P_E along the various density functionals stem mainly from the variations in the exchange part of the functional and to a lesser extent from the correlation part (see Table S4 and Refs. 11,12). Thus, changes in the correlation part lead to variations of 0.5 kcal/mol or less for the overall performance P_E (compare OPBE, OPerdew, OLYP entries in Table S4), while changes in the exchange part may lead to differences of up to 3.0 kcal/mol (compare OPBE, revPBE, RPBE, mPBE, PBE, PBE0 in Table S4). For individual energy terms, these differences may be even larger, as witnessed in the MAD value for the overall barrier for the OPBE, revPBE, RPBE, mPBE, PBE, PBE0 functionals (that all use PBE correlation, but differ in the exchange part), which are found in the range from 2.7 to 10.0 kcal/mol for the CC//CC set (see Table S4).

Geometry Optimization for CC//CC Set

The reference data of the CC//CC set have also been used for comparing the performance of DFT functionals for obtaining the geometry of stationary points; papers **A1** and **A8** were not included here because the basis sets in the original papers are not appropriate compared with the other papers in the CC//CC set, e.g., the best hybrid functional has an overall performance P_E value of 2.9 kcal/mol for paper **A1** (see Table 2), which is roughly three to four times as large as the value for papers **A2–A6** (see Table 2).

For each stationary point, the most reliable reference geometry was chosen if more than one is available, and the structure reoptimized with several DFT functionals. Within the ADF program, analytical gradients are available only for LDA and GGA functionals. Therefore, the QUILD program has been used for studying the geometries from meta-GGA and hybrid functionals. Geometry optimization is very time consuming for these two classes of density functionals because gradients are obtained by numerical differentiation of the energies. Therefore, only the best meta-GGA (OLAP3) and hybrid functional (mPBE0KCIS) from the first part (evaluation of the energies) have been taken into account, together with almost all GGA functionals available within ADF (PW91 was not considered because it should give results similar to PBE[26,37]).

The results of our density-functional geometry optimizations are collected in Table6, which is divided into three parts. The first deals with the deviations of bonds from the reference CCSD(T) data, and is subdivided into deviations for the reactants or products ($R_{R,P}$), for reactant or product complexes ($R_{RC,PC}$) and for transition structures (R_{TS}). The second part concerns the deviation of angles and is subdivided in a similar fashion. Finally, the product of the deviations for the bonds and the angles is taken as a measure for the overall performance P_G regarding geometry optimizations:

$$P_G = \mathrm{MAD}(R) \times \mathrm{MAD}(\theta) \quad (2)$$

The most striking feature from Table 6 is the difference between the recent GGA (OLYP, OPBE) and standard (LDA, BP86, BLYP) functionals. Where the former show an overall performance P_G [see eq. (2)] of 0.03 (OLYP) and 0.04 (OPBE), standard functionals show P_G values starting from 0.27 (RevPBE) to 0.72

for BLYP. This difference results from the bonds (where the MAD values of the standard functionals are up to twice as large as those for the recent functionals that involve the OPTX exchange functional), but mostly from the angles for which the MAD values for standard functionals are at least five times and sometimes up to almost 10 times larger than those from OLYP and OPBE.

Interestingly, the best GGA functionals perform better than the meta-GGA and hybrid functionals (see Table 6). For example, although mPBE0KCIS gives a smaller deviation for the bonds (0.05 Å *vs.* 0.06 Å, see Table 6), the deviation for the angles is twice as large (1.3° *vs.* 0.6/0.7°). On the other hand, while OLAP3 shows a smaller deviation for the angles (0.5°), the deviation for the bonds is twice as large (0.13 Å). Therefore, the overall performance P_G of the meta-GGA and hybrid functionals is about twice as large as that for the best GGA functionals (see Table 6).

Conclusions

We have evaluated the performance of 50 popular (and less popular) density functionals, covering LDA, GGA, meta-GGA, and hybrid DFT, for describing a broad spectrum of 64 S_N2 reactions, by comparing the DFT results with highly correlated ab initio benchmark data (mainly CCSD(T)) from the literature[13,15,55–75] for PES and geometries of stationary points.

The best DFT approaches in this study perform strikingly well in reproducing the benchmark data of the vast set of test reactions. The best GGA, meta-GGA, and hybrid functionals are OPBE, OLAP3, and mPBE0KCIS, respectively, with overall performance P_E values [see eq. (1) for definition] of 2.9, 2.3, and 2.2 kcal/mol. The MAD for the central/overall barriers are 3.7/2.7 (OPBE), 2.1/2.2 (OLAP3), and 1.9/2.7 (mPBE0KCIS) kcal/mol respectively. Note that the hybrid functionals perform only marginally better than the pure functionals, with the popular B3LYP (4.5/6.0 kcal/mol) even performing worse than OPBE. More detailed analyses suggest that the good performance of OLAP3 and mPBE0KCIS is probably fortuitous. In general, it is the exchange part and not the correlation part of the energy functional (causing variations in overall performance P_E [see eq. (1) for definition] of up to 3.0 *vs.* 0.5 kcal/mol) that determines the accuracy of the DFT method for our model reactions, in line with previous studies.[11,12]

The same GGA functionals that performed best for the energies (OPBE, OLYP), also perform best for the geometries with MADs in bond distances and angles of 0.06 Å and 0.6°, leading to overall performance P_G values [see eq. (2) for definition] of 0.03 and 0.04. This is significantly better than the P_G values of regular (i.e., no OPTX exchange) GGA functionals (P_G values 0.27–0.72), the best meta-GGA (OLAP3: P_G value 0.07), and the best hybrid DFT (mPBE0KCIS: P_G value 0.06).

In view of the much higher computational efficiency of GGAs compared with meta-GGAs and hybrid functionals, let alone coupled cluster, we recommend the use of accurate GGAs such as OPBE or OLYP for studying S_N2 reactions. If the accuracy should be taken to the limit in a computationally still efficient manner, we recommend to use mPBE0KCIS/QZ4P in a single-point fashion using OLYP/QZ4P geometries (mPBE0KCIS/QZ4P//OLYP/QZ4P).

Supporting Information

Tables with reference energy data, mean absolute deviations for all density functionals per set of reference data (A, B and C); Cartesian coordinates of all intermediate structures used in this study.

Acknowledgments

The authors thank L. Angel, S. Bachrach, W. Hase, D. Mulhearn, Y. Ren, L. Sun, and E. Uggerud for providing additional data not contained in the original sources.

References

1. Watson, J. D. DNA: The Secret of Life; New York: Random House, 2004.
2. Fonseca Guerra, C.; Bickelhaupt, F. M. Angew Chem Int Ed 1999, 38, 2942.
3. Fonseca Guerra, C.; Bickelhaupt, F. M.; Snijders, J. G.; Baerends, E. J. Chem-Eur J 1999, 5, 3581.
4. Fonseca Guerra, C.; Bickelhaupt, F. M.; Snijders, J. G.; Baerends, E. J. J Am Chem Soc 2000, 122, 4117.
5. Fonseca Guerra, C.; Bickelhaupt, F. M. Angew Chem Int Ed 2002, 41, 2092.
6. Hagenbuch, P.; Kervio, E.; Hochgesand, A.; Plutowski, U.; Richert, C. Angew Chem Int Ed 2005, 44, 6588.
7. Laerdahl, J. K.; Uggerud, E. Int J Mass Spectrom 2002, 214, 277.
8. Koch, W.; Holthausen, M. C. A Chemist's Guide to Density Functional Theory; Wiley-VCH: Weinheim, 2000.
9. Parr, R. G.; Yang, W. Density Functional Theory of Atoms and Molecules; Oxford University Press: New York, 1989.
10. Dreizler, R.; Gross, E. Density Functional Theory; Plenum Press: New York, 1995.
11. Grüning, M.; Gritsenko, O.; Baerends, E. J. J Phys Chem A 2004, 108, 4459.
12. Gritsenko, O. V.; Ensing, B.; Schipper, P. R. T.; Baerends, E. J. J Phys Chem A 2000, 104, 8558.
13. Bento, A. P.; Solà, M.; Bickelhaupt, F. M. J Comput Chem 2005, 26, 1497.
14. Swart, M.; Ehlers, A. W.; Lammertsma, K. Mol Phys 2004, 102, 2467.
15. Gonzales, J. M.; Cox, R. S., III; Brown, S. T.; Allen, W. D.; Schaefer H. F., III. J Phys Chem A 2001, 105, 11327.
16. Kormos, B. L.; Cramer, C. J. J Phys Org Chem 2002, 15, 712.
17. Poater, J.; Solà, M.; Duran, M.; Robles, J. Phys Chem Chem Phys 2002, 4, 722.
18. Zhao, Y.; González-García, N.; Truhlar, D. G. J Phys Chem A 2005, 109, 2012.
19. Becke, A. D. Phys Rev A 1988, 38, 3098.
20. Perdew, J. P. Phys Rev B, 1986, 33, 8822. Erratum: ibid., 8834, 7406.
21. Stephens, P. J.; Devlin, F. J.; Chabalowski, C. F.; Frisch, M. J. J Phys Chem 1994, 45, 11623.
22. Zhao, Y.; Schultz, N. E.; Truhlar, D. G. J Chem Theor Comput 2006, 2, 364.
23. Baerends, E. J.; Autschbach, J.; Bérces, A.; Bo, C.; Boerrigter, P. M.; Cavallo, L.; Chong, D. P.; Deng, L.; Dickson, R. M.; Ellis, D. E.; Fan, L.; Fischer, T. H.; Fonseca Guerra, C.; van Gisbergen, S. J. A.; Groeneveld, J. A.; Gritsenko, O. V.; Grüning, M.; Harris, F. E.; van den Hoek, P.; Jacobsen, H.; van Kessel, G.; Kootstra, F.;

van Lenthe, E.; McCormack, D. A.; Osinga, V. P.; Patchkovskii, S.; Philipsen, P. H. T.; Post, D.; Pye, C. C.; Ravenek, W.; Ros, P.; Schipper, P. R. T.; Schreckenbach, G.; Snijders, J. G.; Solà, M.; Swart, M.; Swerhone, D.; te Velde, G.; Vernooijs, P.; Versluis, L.; Visser, O.; van Wezenbeek, E.; Wiesenekker, G.; Wolff, S. K.; Woo, T. K.; Ziegler, T. SCM: Amsterdam, 2004.
24. te Velde, G.; Bickelhaupt, F. M.; Baerends, E. J.; Fonseca Guerra, C.; van Gisbergen, S. J. A.; Snijders, J. G.; Ziegler, T. J Comput Chem 2001, 22, 931.
25. van Lenthe, E.; Baerends, E. J. J Comput Chem 2003, 24, 1142.
26. Swart, M.; Snijders, J. G. Theor Chem Acc 2003, 110, 34. Erratum: ibid 111, 156.
27. Swart, M.; Groenhof, A. R.; Ehlers, A. W.; Lammertsma, K. J Phys Chem A 2004, 108, 5479.
28. de Jong, G. Th.; Bickelhaupt, F. M. J Chem Theor Comput 2006, 2, 322.
29. de Jong, G. Th.; Bickelhaupt, F. M. J Phys Chem A 2005, 109, 9685.
30. de Jong, G. Th.; Geerke, D. P.; Diefenbach, A.; Solà, M.; Bickelhaupt, F. M. J Comput Chem 2005, 26, 1006.
31. de Jong, G. Th.; Geerke, D. P.; Diefenbach, A.; Bickelhaupt, F. M. Chem Phys 2005, 313, 261.
32. Vosko, S. H.; Wilk, L.; Nusair, M. Can J Phys 1980, 58, 1200.
33. Swart, M.; Bickelhaupt, F. M. Amsterdam, 2005.
34. Swart, M.; Bickelhaupt, F. M. Int J Quant Chem 2006, 106, 2536.
35. Perdew, J. P.; Ruzsinszky, A.; Tao, J. M.; Staroverov, V. N.; Scuseria, G. E.; Csonka, G. I. J Chem Phys 2005, 123, 062201.
36. Lee, C.; Yang, W.; Parr, R. G. Phys Rev B 1988, 37, 785.
37. Perdew, J. P.; Burke, K.; Ernzerhof, M. Phys Rev Lett 1996, 77, 3865. Erratum 3878, 1396.
38. Hamprecht, F. A.; Cohen, A. J.; Tozer, D. J.; Handy, N. C. J Chem Phys 1998, 109, 6264.
39. Boese, A. D.; Handy, N. C. J Chem Phys 2001, 114, 5497.
40. Boese, A. D.; Doltsinis, N. L.; Handy, N. C.; Sprik, M. J Chem Phys 2000, 112, 1670.
41. Staroverov, V. N.; Scuseria, G. E.; Tao, J.; Perdew, J. P. J Chem Phys 2003, 119, 12129.
42. Handy, N. C.; Cohen, A. J. Mol Phys 2001, 99, 403.
43. Baker, J.; Pulay, P. J Chem Phys 2002, 117, 1441.
44. Xu, X.; Goddard, W. A., III. J Phys Chem A 2004, 108, 8495.
45. Proynov, E. I.; Sirois, S.; Salahub, D. R. Int J Quant Chem 1997, 64, 427.
46. Filatov, M.; Thiel, W. Mol Phys 1997, 91, 847.
47. van Voorhis, T.; Scuseria, G. J Chem Phys 1998, 109, 400.
48. Krieger, J. B.; Chen, J.; Iafrate, G. J.; Savin, A. In Electron Correlations and Materials Properties; Gonis, A.; Kioussis, N., Eds.; Plenum: New York, 1999.
49. Becke, A. D. J Chem Phys 2000, 112, 4020.
50. Tao, J. M.; Perdew, J. P.; Staroverov, V. N.; Scuseria, G. E. Phys Rev Lett 2003, 91, 146401.
51. Nibbering, N. M. M. Adv Phys Org Chem 1988, 24, 1.
52. Bickelhaupt, F. M. Mass Spectrom Rev 2001, 20, 347.
53. Bickelhaupt, F. M.; Baerends, E. J.; Nibbering, N. M. M. Chem–Eur J 1996, 2, 196.
54. Bickelhaupt, F. M. J Comput Chem 1999, 20, 114.
55. Gonzales, J. M.; Pak, C.; Cox, R. S.; Allen, W. D.; Schaefer, H. F. III; Császár, A. G.; Tarczay, G. Chem–Eur J 2003, 9, 2173.
56. Angel, L. A.; Ervin, K. M. J Phys Chem A 2001, 105, 4042.
57. Angel, L. A.; Ervin, K. M. J Phys Chem A 2004, 108, 9827.
58. Angel, L. A.; Garcia, S. P.; Ervin, K. M. J Am Chem Soc 2002, 124, 336.
59. Bachrach, S. M.; Mulhearn, D. C. J Phys Chem 1996, 100, 3535.
60. Borisov, Y. A.; Arcia, E. E.; Mielke, S. L.; Garrett, B. C.; Dunning, T. H., Jr. J Phys Chem A 2001, 105, 7724.
61. Botschwina, P. Theor Chem Acc 1998, 99, 426.
62. Botschwina, P.; Horn, M.; Seeger, S.; Oswald, R. Ber Bunsenges Phys Chem 1997, 101, 387.
63. Glukhovtsev, M. N.; Pross, A.; Radom, L. J Am Chem Soc 1995, 117, 2024.
64. Glukhovtsev, M. N.; Pross, A.; Radom, L. J Am Chem Soc 1995, 117, 9012.
65. Lee, I.; Kim, C. K.; Sohn, C. K.; Li, H. G.; Lee, H. W. J Phys Chem A 2002, 106, 1081.
66. Matsubara, H.; Horvat, S. M.; Schiesser, C. H. Org Biomol Chem 2003, 1, 1199.
67. Parthiban, S.; de Oliveira, G.; Martin, J. M. L. J Phys Chem A 2001, 105, 895.
68. Schmatz, S.; Botschwina, P.; Hauschildt, J.; Schinke, R. J Chem Phys 2001, 114, 5233.
69. Schmatz, S.; Botschwina, P.; Stoll, H. Int J Mass Spectrom 2000, 201, 277.
70. Sun, L.; Song, K.; Hase, W. L.; Sena, M.; Riveros, J. M. Int J Mass Spectrom 2003, 227, 315.
71. Uggerud, E. J Chem Soc Perkin Trans 1999, 2, 1459.
72. Wang, H.; Hase, W. L. J Am Chem Soc 1997, 119, 3093.
73. Wladkowski, B. D.; Allen, W. D.; Brauman, J. I. J Phys Chem 1994, 98, 13532.
74. Xiong, Y.; Zhu, H.; Ren, Y. J Mol Struct (Theochem) 2003, 664-665, 279.
75. Yu, Z.-X.; Wu, Y.-D. J Org Chem 2003, 68, 6049.
76. Helgaker, T.; Gauss, J.; Jørgensen, P.; Olsen, J. J Chem Phys 1997, 106, 6430.